LETTERS

A scaling law for slow earthquakes

Satoshi Ide[1], Gregory C. Beroza[2], David R. Shelly[2] & Takahiko Uchide[1]

Recently, a series of unusual earthquake phenomena have been discovered, including deep episodic tremor[1], low-frequency earthquakes[2], very-low-frequency earthquakes[3], slow slip events[4] and silent earthquakes[5–9]. Each of these has been demonstrated to arise from shear slip, just as do regular earthquakes, but with longer characteristic durations and radiating much less seismic energy. Here we show that these slow events follow a simple, unified scaling relationship that clearly differentiates their behaviour from that of regular earthquakes. We find that their seismic moment is proportional to the characteristic duration and their moment rate function is constant, with a spectral high-frequency decay of f^{-1}. This scaling and spectral behaviour demonstrates that they can be thought of as different manifestations of the same phenomena and that they comprise a new earthquake category. The observed scale dependence of rupture velocity for these events can be explained by either a constant low-stress drop model or a diffusional constant-slip model. This new scaling law unifies a diverse class of slow seismic events and may lead to a better understanding of the plate subduction process and large earthquake generation.

In recent years, an expanding variety of unusual earthquakes have been discovered. Since the 1990s, silent earthquakes[5–9], some with moment magnitude M_w as large as 7.5, have been discovered through Global Positioning System and strain meter measurements, with durations ranging from minutes to months. In particular, a dense network of high-sensitivity seismometers and tiltmeters maintained by the National Research Institute for Earth Science and Disaster Prevention, Hi-net[10], has successively led to the discovery of low-frequency earthquakes (LFE)[2], low-frequency tremor[1], and slow-slip events (SSE)[4] in essentially the same place along the Nankai trough in western Japan. Similar phenomena have been found in the Cascadia subduction zone[11]. These episodes have come to be referred to as episodic tremor and slip (ETS). A different type of event, known as very-low-frequency earthquakes (VLF), with characteristics between those of LFEs and SSEs, has now also been discovered in western Japan[3]. Despite the variety of names, these events occur at the same time and in the same place, which suggests a close relationship and perhaps a common origin. A unifying characteristic of these events is that they have much longer durations than ordinary earthquakes of comparable seismic moment. For this reason, we refer to them all as slow earthquakes.

Figure 1 shows examples of these events around Shikoku, Japan. Both LFEs and low-frequency tremor occur in a belt-like zone that follows the 35-km iso-depth curves of the top of the Philippine Sea plate[12]. Although LFEs are isolated in time and tremor is continuous, these two phenomena radiate seismic waves with very similar waveforms and spectra, predominantly at frequencies of 1–8 Hz, suggesting that the underlying physical mechanism is the same[13]. LFEs appear to be shear slip on the plate interface because of their distribution on an $\sim 20°$ dipping plane that corresponds to the dip of Philippine Sea plate subduction[14] and because they have a sense of

deformation consistent with relative plate motion[15]. SSEs are detected by tiltmeters and co-located with LFEs and tremor. Two types of SSEs have been reported, long-term SSEs of $M_w \approx 7$ and short-term SSEs of $M_w \approx 6$. A long-term SSE in 2003 continued for about five months, while short-term SSEs occur over 3–7-day periods[4]. VLFs are weak signals found in both borehole accelerometer (tiltmeter) records and in broadband seismograms. Their locations overlap those of the other phenomena, but with a characteristic frequency of 0.02–0.05 Hz (ref. 3). The fault slip models of SSEs and the moment tensors of VLFs are consistent with the mechanisms of LFEs, past megathrust earthquakes[16], and global plate motion[17]. Therefore it appears that this entire range of phenomena represents shear slip on the plate interface.

Table 1 and Fig. 2 summarize characteristic quantities of low-frequency tremor, LFEs, VLFs and SSEs in the Nankai trough, together with those of ETS in the Cascadia subduction zone and some silent earthquakes. Except for two silent earthquakes that occurred along the Japan trench[6,7] in places where tremor activity is not reported, we find a clear proportionality between the characteristic duration T (in units of seconds) and the seismic moment, a measure of the size of final fault motion, M_0 (in units of N m):

$$M_0 \approx T \times 10^{12–13} \qquad (1)$$

which is different from the scaling of regular (in the sense of 'normal') earthquakes in subduction zones[18]:

$$M_0 \approx T^3 \times 10^{15–16} \qquad (2)$$

Since the discovery of silent earthquakes, the possibility of a gap between large, regular earthquakes and silent earthquakes has become apparent. We propose that this gap is there because the two types of earthquake represent different modes of slip propagation, and that the only events capable of filling the gap would be a composite of two rupture modes.

If we assume that the proportionality between seismic moment and characteristic time holds at all times during an earthquake, then the seismic moment rate function $\dot{M}_0(t)$ would be constant until the event's termination. Approximately constant moment rates have been observed at large scales, both in the Nankai subduction zone[8] and in numerical simulations[19]. Far-field seismic displacement $u(t)$ is proportional to $\dot{M}_0(t)$, so we would expect a box-car displacement pulse for these events. The Fourier amplitude spectrum of a box-car function of duration T is proportional to $\sin(\pi fT)/(\pi fT)$, where f is frequency. This spectrum is asymptotically flat at low-frequency and falls asymptotically as f^{-1} at high-frequency. Although the actual moment rate function in detail will be more complex than this, a seismic source with fairly abrupt onset and termination compared to variations in moment rate should lead to a spectrum that is similar.

This spectral behaviour differs from that observed for regular earthquakes, which exhibit f^{-2} spectral decay at high frequency

---

[1]Department of Earth and Planetary Science, University of Tokyo, Hongo 7-3-1, Bunkyo-ku, Tokyo 113-0033, Japan. [2]Department of Geophysics, 397 Panama Mall, Stanford University, Stanford, California 94305-2215, USA.
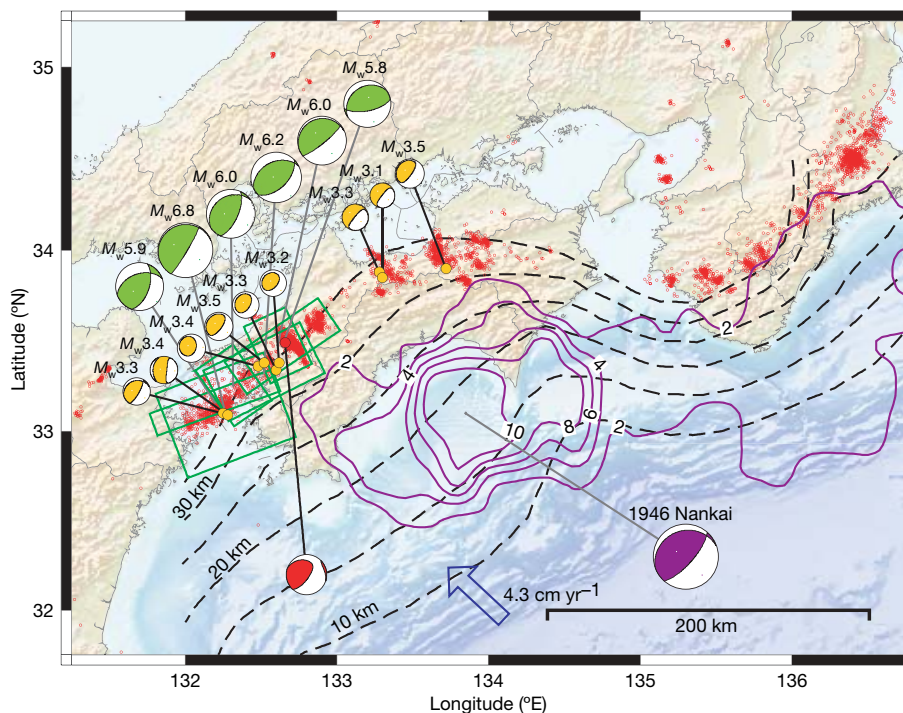
Figure 1 | Various types of earthquakes and their mechanisms along the Nankai trough, western Japan. Red dots represent LFE locations determined by the Japan Meteorological Agency[2]. Red and orange 'beach balls' show the mechanism of LFEs[15] and VLFs[3], respectively. Green rectangles and beach balls show fault slip models of SSE[4]. Purple contours and the purple beach ball show the slip distribution[31] (in metres) and focal mechanism[16] of the 1946 Nankai earthquake ($M_w = 8$). The top of the Philippine Sea plate is shown by dashed contours[12]. The blue arrow represents the direction of relative plate motion in this area[17].

(Fig. 3a). The spectra of VLFs, LFEs and tremor all follow f^{-1} decay at high frequency (Fig. 3b, c), which suggests a constant moment rate over these smaller length scales too. The f^{-1} decay is also supported by the difference in slope between stacked spectra of LFEs and regular earthquakes[13]. That is, the spectra of these events are consistent with the overall proportionality between released seismic moment and elapsed time during the slow earthquakes shown in Fig. 2. Figure 3b also suggests that the observed characteristic size of VLFs and LFEs may be due to the strong background noise from microseisms, which inhibits the discovery of events with sizes intermediate between VLFs and LFEs. If tremor, LFEs, VLFs and SSEs are all governed by the same process in the same area, the difference between them corresponds only to the final size that an event achieves. Our scaling relations suggest that we should expect slower earthquakes of $M_w \approx 4$–5 with durations of tens of minutes to an hour in the same area. Such events have not yet been observed, but may be detectable on sensitive broad-band instruments, if noise levels are sufficiently low.

The discovery of this scaling relation leads to the question of what controls these processes. Seismic moment can be written using the characteristic dimension of the fault plane L and the average slip amount D:

$$M_0 = \mu D L^2 \qquad (3)$$

where μ is the rigidity. The slip amounts of SSEs and ETSs are of the order of centimetres. Because the average slip amounts of smaller events are unknown, we consider two mechanisms with different scalings of D. First, we assume that D is proportional to L as in regular earthquakes. Stress drop $\Delta\sigma \approx \mu D/L$ is about 10 kPa for the large slow earthquakes in Table 1 if μ is 30 GPa, so this assumption leads to a constant stress drop of 10 kPa. This is smaller by about two orders of magnitude than that of regular earthquakes and we refer to this assumption as the low-stress drop model. The constant-stress drop assumption, together with equations (1) and (3), gives the relation

Table 1 | Source parameters of slow earthquakes

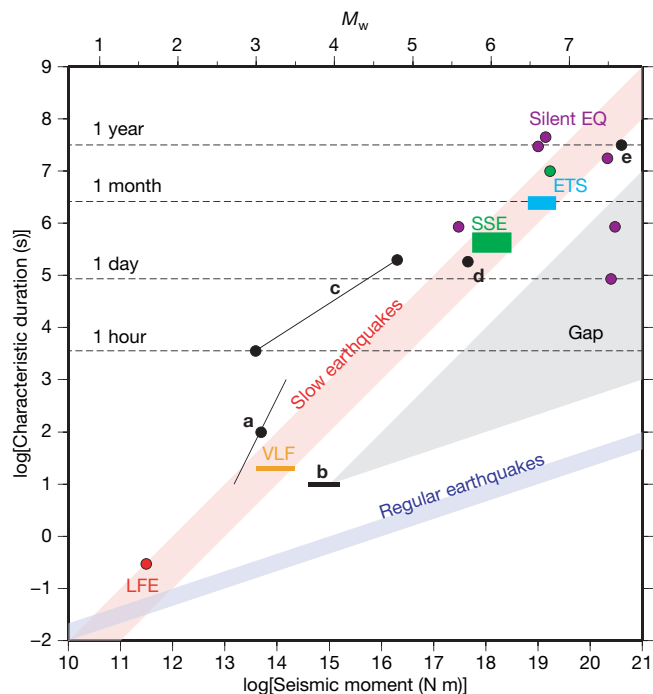| Type	M_0 (N m)	T (s)	Characteristic frequency (Hz)	D (m)	L (m)	Area
Low-frequency tremor			1–8			Nankai trough
LFE	3×10^{11}	0.3	1–8			Nankai trough[15]
VLF	0.4–2.2×10^{14}	~20	0.02–0.05			Nankai trough[3]
SSE short-term	0.6–2.8×10^{18}	3–6×10^5		0.008–0.026	3–5×10^4	Nankai trough[4]
SSE long-term	1.7×10^{19}	10^7		0.11	5–7×10^4	Nankai trough[4]
Silent earthquakes	1.1×10^{19}	3×10^7		<0.18	6×10^4	Nankai trough[5]
	1.4×10^{19}	5×10^7		0.2	10^5	Nankai trough[8]
	1–4×10^{20}	10^5				Northeast Japan[6]
	3×10^{20}	10^6				Northeast Japan[7]
	2.2×10^{20}	1.7×10^7		0.1	2–5×10^5	Mexico[9]
ETS	0.7–2.0×10^{19}	2–3×10^6		0.02	1.5×10^5	Cascadia[11]
Afterslip	4.2×10^{20}	3×10^7		0.7–0.9	10^5	Northeast Japan[27]
Shallow VLF	0.4–1.6×10^{15}	~ 10	0.08–0.24			Northeast Japan[26]
Slow slip (creep)	2×10^{16}	2×10^5		0.03–0.1	5,000	San Andreas[22]
	4.4×10^{13}	3,600				San Andreas[21]
Slow slip in volcano	6.8×10^{17}	1.9×10^5		>0.015	1.5×10^4	Hawaii[25]
Aseismic fault	4.9×10^{13}	100			250	Italy[23,24]

between L and T:

$$L^3 = C_1 T \qquad (4)$$

where $C_1 \approx 3 \times 10^8 \, \mathrm{m}^3 \, \mathrm{s}^{-1}$. This relation predicts that the characteristic propagation velocity for these events L/T is proportional to $1/L^2$; it is fast for shorter lengths and slow for longer lengths, which is consistent with the observed propagation velocity of these slow earthquakes. When $L \approx 100$ km, the characteristic velocity is about 5–15 km day^{-1} (~ 0.1 m s^{-1}) for ETS and SSE, while tremor propagates for about 10 km at a rupture velocity of about 45 km h^{-1} (~ 10 m s^{-1})[13]. Although the above assumption describes the observed size-dependent rupture velocity, the physical mechanism that leads to this dependence is unclear.

As an alternative model, we next assume that the slip amounts are almost constant, and limited by the accumulated plate motion since the last event. That is, we assume they are comparable to the value of slip observed in SSEs and ETSs. Assuming a constant D for all events, equations (1) and (3) lead to a relation between L and T:

$$L^2 = C_2 T \qquad (4)$$

where the constant C_2 is about $10^4 \, \mathrm{m}^2 \, \mathrm{s}^{-1}$ if $D = 0.01$ m and μ is 30 GPa. Because this is of the form of a scaling relation for diffusion-controlled physical phenomena[20] with a diffusion constant of C_2, we refer to this relationship as the diffusional earthquake model. In this model, the stress drop $\Delta\sigma \approx \mu D/L$ is larger for an initial small event and decreases with increasing event size. The propagation velocity L/T decreases proportionally to $1/L$, as the stress concentration decreases. Equation (4) explains the rupture velocity of 0.1 m s^{-1}

for $L \approx 100$ km, while the characteristic velocity of 1 m s^{-1} for $L \approx 10$ km is somewhat slower than observed.

It is interesting to note that the scaling relations of slow and regular earthquakes intersect at about $M_w \approx 1$ ($M_0 \approx 10^{11}$ N m), near the minimum size of both LFEs and typically detected regular earthquakes. In the low-stress earthquake model, the rupture propagation velocity would be ~ 10 km s^{-1}, which is unphysical because it would be faster than the elastic wave speed. The diffusional earthquake model predicts a rupture velocity of 1 km s^{-1} with the stress drop of about 20 MPa, which is not impossible, but in the case of stress drop is much higher than observed for regular earthquakes. These physically unrealizable conditions may limit the smallest scale of the slow earthquakes to the magnitude of LFEs or the slightly smaller tremor. The lack of VLFs or SSEs during some LFE and tremor episodes suggests that a single LFE or slightly smaller events may be an elementary event that marks the smallest slow earthquake.

As more and more earthquakes that fit into the category of slow earthquakes are identified, it is natural that they would initially be considered as different and perhaps unrelated phenomena. In this regard, we note that there are other earthquakes falling into this category that occur in other environments. Transient slip events have
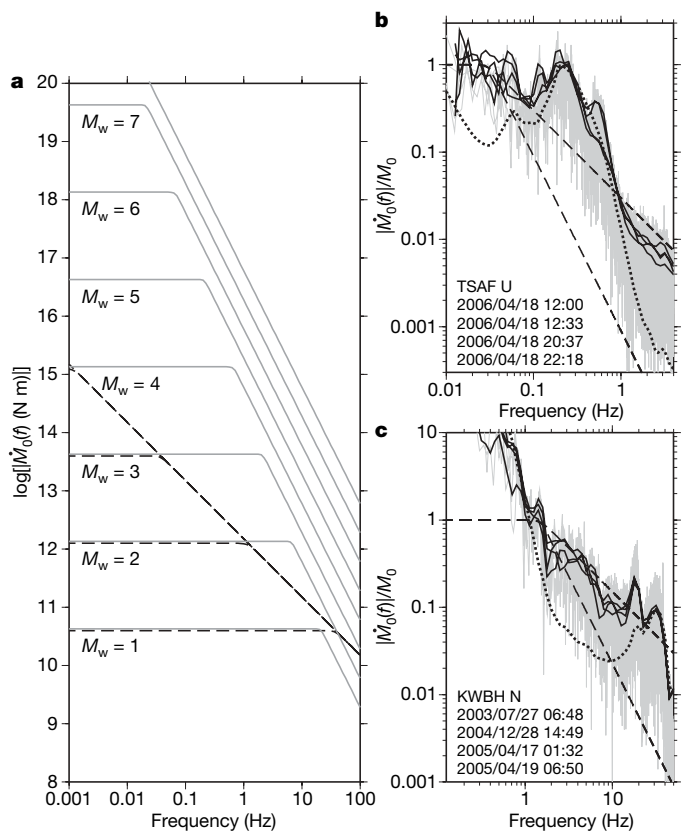

Figure 2 | Comparison between seismic moment and the characteristic duration of various slow earthquakes in Table 1. LFE (red), VLF (orange), and SSE (green) occur in the Nankai trough while ETS (light blue) occur in the Cascadia subduction zone. These follow a scaling relation of $M_0 \propto t$, for slow earthquakes. Purple circles are silent earthquakes. Black symbols are slow events listed in the bottom half of Table 1. **a,** Slow slip in Italy[23,24], representing a typical event (circle) and proposed scaling (line). **b,** VLF earthquakes in the accretionary prism of the Nankai trough[26]. **c,** Slow slip and creep in the San Andreas Fault[21,22]. **d,** Slow slip beneath Kilauea volcano[25]. **e,** Afterslip of the 1992 Sanriku earthquake[27]. Typical scaling relation for shallow interplate earthquakes is also shown by a thick blue line.

Figure 3 | Characteristics of moment rate spectrum of slow earthquakes. a, Scaling of moment rate spectrum of slow earthquakes (black dashed lines) and regular earthquakes (grey lines) for different magnitudes. **b,** An example of displacement spectrum (moment rate spectrum) of a VLF event. Original (grey) and averaged (thick black) spectra are shown. The seismograms represent the up–down (U) component at station TSAF for four VLFs that occurred on 18 April 2006 at the times shown in Table S1 of ref. 3. The noise level is shown by the dotted line. There is a large peak due to microseisms between 0.1–1 Hz. **c,** Same as **b** but for an LFE. The seismograms represent the north–south (N) component at station KWBH for the reference LFE in ref. 15 and three LFEs that occurred nearby, at the times shown. (Note that the frequency axes in **b** and **c** are different.) For both VLF and LFE, spectra are well explained with a slope of f^{-1} at high frequency rather than f^{-2} (dashed curves). We corrected for the effect of attenuation, assuming that these waves are S waves and $Q = 200$. Peaks above 10 Hz probably show amplification due to the site and/or instrument characteristics.

been discovered along the San Andreas Fault, California[21,22], along an inactive fault in Italy[23,24], beneath Kilauea volcano, Hawaii[25], and within the shallow accretionary prism along the Japan trench[26]. The afterslip of large earthquakes, such as that observed after the 1994 Sanriku earthquake[27], may also be regarded as a kind of silent slip, and thus fall into this category. The duration and seismic moment of these events all fall in or around the diffusional limb of the scaling law shown in Fig. 2. The substantial scatter in this log-arithmic plot indicates that other physical phenomena may well be important, but the difference in scaling between regular and slow earthquakes defines two distinct populations, and is likely to be a useful starting point for classifying different phenomena.

Important questions remain about the physical mechanism behind both the low-stress drop and the diffusional earthquake models. In the slow-earthquake zone of the Nankai trough, the existence of fluid is suggested by seismic wave tomography[14], which suggests that the introduction of fluid and its subsequent diffusion is the underlying mechanism. Rate- and state-dependent friction laws[28,29] can also lead to propagation of slow slip without fluids[19,30]. Further studies will address these questions and undoubtedly refine the simplifications made in our interpretation; however, the scaling law for slow earthquakes unifies a seemingly diverse class of unusual, recently discovered seismic events. Understanding these earthquakes should lead to new insights into the physics of plate subduction and in assessing the probability of future large earthquakes.

1. Obara, K. Nonvolcanic deep tremor associated with subduction in southwest Japan. *Science* 296, 1679–1681 (2002).
2. Katsumata, A. & Kamaya, N. Low-frequency continuous tremor around the Moho discontinuity away from volcanoes in the southwest Japan. *Geophys. Res. Lett.* 30, doi:10.1029/2002GL015981 (2003).
3. Ito, Y., Obara, K., Shiomi, K., Sekine, S. & Hirose, H. Slow earthquakes coincident with episodic tremors and slow slip events. *Science* 26, 503–506 (2006).
4. Hirose, H. & Obara, K. Repeating short- and long-term slow slip events with deep tremor activity, around the Bungo channel region, southwest Japan. *Earth Planets Space* 57, 961–972 (2005).
5. Hirose, H., Hirahara, K., Kimata, F., Fujii, N. & Miyazaki, S. A slow thrust slip event following the two 1996 Hyuganada earthquakes beneath the Bungo Channel, southwest Japan. *Geophys. Res. Lett.* 26, 3237–3240 (1999).
6. Kawasaki, I. *et al.* The 1992 Sanriku-oki, Japan, ultra-slow earthquake. *J. Phys. Earth* 43, 105–116 (1995).
7. Kawasaki, I., Asai, Y. & Tamura, Y. Space-time distribution of interplate moment release including slow earthquakes and seismo-geodetic coupling in the Sanriku-oki region along the Japan trench. *Tectonophysics* 330, 267–283 (2001).
8. Ozawa, S. *et al.* Detection and monitoring of ongoing aseismic slip in the Tokai region, central Japan. *Science* 298, 1009–1012 (2002).
9. Kostoglodov, V. *et al.* A large silent earthquake in the Guerrero seismic gap, Mexico. *Geophys. Res. Lett.* 30, doi:10.1029/2003GL017219 (2003).
10. Obara, K., Kasahara, K., Hori, S. & Okada, Y. A densely distributed high-sensitivity seismograph network in Japan: Hi-net by National Research Institute for Earth Science and Disaster Prevention. *Rev. Sci. Instrum.* 76, doi:10.1063/1.1854197 (2005).
11. Dragert, H., Wang, K. & Rogers, G. Geodetic and seismic signatures of episodic tremor and slip in the northern Cascadia subduction zone. *Earth Planets Space* 56, 1143–1150 (2004).
12. Baba, T., Tanioka, T., Cummins, P. R. & Uhira, K. The slip distribution of the 1946 Nankai earthquake estimated from tsunami inversion using a new plate model. *Phys. Earth Planet. Inter.* 132, 59–73 (2002).
13. Shelly, D. R., Beroza, G. C. & Ide, S. Non-volcanic tremor and low frequency earthquake swarms. *Nature* 446, 305–307 (2007).
14. Shelly, D. R., Beroza, G. C., Ide, S. & Nakamula, S. Low-frequency earthquakes in Shikoku, Japan, and their relationship to episodic tremor and slip. *Nature* 442, 188–191 (2006).
15. Ide, S., Shelly, D. R. & Beroza, G. C. The mechanism of deep low frequency earthquakes: further evidence that deep non-volcanic tremor is generated by shear slip on the plate interface. *Geophys. Res. Lett.* 34, doi:10.1029/2006GL028890 (2007).
16. Ando, M. A fault model of the 1946 Nankaido earthquake derived from tsunami data. *Phys. Earth Planet. Inter.* 28, 320–336 (1982).
17. DeMets, C., Gordon, R. G., Argus, D. F. & Stein, S. Effect of recent revisions to the geomagnetic reversal time scale on estimates of current plate motions. *Geophys. Res. Lett.* 21, 2191–2194 (1994).
18. Houston, H. Influence of depth, focal mechanism, and tectonic setting on the shape and duration of earthquake source time functions. *J. Geophys. Res.* 106, 11137–11150 (2001).
19. Shibazaki, B. & Iio, Y. On the physical mechanism of silent slip events along the deeper part of the seismic zone. *Geophys. Res. Lett.* 30, doi:10.1029/2003GL017047 (2003).
20. Barenblatt, G. I. *Scaling, Self-similarity, and Intermediate Asymptotics* (Cambridge Univ. Press, Cambridge, UK, 1996).
21. Gladwin, M. T., Gwyther, R. L., Hart, R. H. G. & Brechenridge, K. S. Measurements of the strain field associated with episodic creep events on the San Andreas fault at San Juan Bautista, California. *J. Geophys. Res.* 99, 4559–4564 (1994).
22. Linde, A. T., Gladwin, M. T., Johnston, M. J. S., Gwyther, R. L. & Bilham, R. G. A slow earthquake sequence on the San Andreas fault. *Nature* 383, 65–67 (1996).
23. Crescentini, L., Amoruso, A. & Scarpa, R. Constraints on slow earthquake dynamics from a swarm in central Italy. *Science* 286, 2132–2134 (1999).
24. Amoruso, A., Crescentini, L., Morelli, A. & Scarpa, R. Slow rupture of an aseismic fault in a seismogenic region of Central Italy. *Geophys. Res. Lett.* 29, doi:10.1029/2002GL016027 (2002).
25. Segall, P., Desmarais, E. K., Shelly, D., Mikilius, A. & Cervelli, P. Earthquakes triggered by silent slip events on Kilauea volcano, Hawaii. *Nature* 442, 71–74 (2006).
26. Ito, Y. & Obara, K. Very low frequency earthquakes within accretionary prisms are very low-stress-drop earthquakes. *Geophys. Res. Lett.* 33, doi:10.1029/2006GL025883 (2006).
27. Heki, K., Miyazaki, S. & Tsuji, H. Silent fault slip following an interplate thrust earthquake at the Japan Trench. *Nature* 386, 595–597 (1997).
28. Dieterich, J. H. Modelling of rock friction: 1 Experimental results and constitutive equations. *J. Geophys. Res.* 84, 2161–2168 (1979).
29. Ruina, A. L. Slip instability and state variable friction laws. *J. Geophys. Res.* 88, 10,359–10,370 (1983).
30. Liu, Y. & Rice, J. R. Aseismic slip transients emerge spontaneously in three-dimensional rate and state modeling of subduction earthquake sequences. *J. Geophys. Res.* 110, doi:10.1029/2004JB003424 (2005).
31. Sagiya, T. & Thatcher, W. Coseismic slip resolution along a plate boundary megathrust: the Nankai Trough, southwest Japan. *J. Geophys. Res.* 104, 1113–1129 (1999).

Author Information Reprints and permissions information is available at www.nature.com/reprints. The authors declare no competing financial interests. Correspondence and requests for materials should be addressed to S.I. (ide@eps.s.u-tokyo.ac.jp).